Far-infrared spectra of alkali germanate glasses and correlation with electrical conductivity

E. I. Kamitsos* and Y. D. Yiannopoulos
Theoretical and Physical Chemistry Institute, National Hellenic Research Foundation, 48 Vass. Constantinou Ave., Athens 116 35, Greece

H. Jain and W. C. Huang
Department of Materials Science and Engineering, Lehigh University, Bethlehem, Pennsylvania 18015
(Received 19 January 1996)

The infrared spectra of $0.20R_2O$-$0.80GeO_2$ (R=Li,Na,K,Rb,Cs) and xRb_2O-$(1-x)GeO_2$ ($0<x\leqslant 0.27$) glasses were measured in the reflectance mode and analyzed by the Kramers-Kronig technique to investigate the nature and composition dependence of metal ion sites in germanate glasses. The deconvolution of the far-infrared profiles showed that in glasses of low alkali content ($x\leqslant 0.075$ for R=Rb) alkali ions occupy one type of sites (M), while for higher alkali contents two types of site (L and H) were found. The ion motion frequencies in these sites are in the order $\nu_L<\nu_M<\nu_H$, and increase with increasing alkali oxide content. Factor group analysis of the alkali motion modes in analogous crystalline germanate compounds showed that the H band in glass can be assigned to ion motion in sites similar to those in the crystal. The low-frequency band (L) was attributed to ion motion in ''secondary'' energetic sites, whose coordination numbers and charge density are correspondingly larger and smaller than their optimum values. The presence of L sites is the cause of the extra absorption exhibited by glasses at low far-infrared frequencies, as compared to the crystals of similar composition. M-type sites were shown to be the precursors of H sites, but for the organization of the latter a minimum alkali oxide content is required. The comparison of activation energies for conductivity calculated on the basis of the free-ion model with observed values suggests that long-range ion movement is probably facilitated along M and H-type sites. [S0163-1829(96)02534-9]

I. INTRODUCTION

The dc conductivity of rubidium germanate glasses has been measured as a function of Rb_2O content.[1,2] The activation energy for ionic conduction, E_σ, was found to exhibit a maximum at ~10 mol % Rb_2O. However, such behavior is not a peculiarity of the rubidium germanate system alone, since similar activation energy maxima have been reported for K-germanate,[3] Li-germanate,[4] and Na-germanate[5] glasses. In any case, the composition dependence of E_σ in germanate glasses is in contrast with the corresponding variation in alkali silicates, where E_σ decreases monotonically with increasing alkali content.

In order to understand the variation of E_σ with Rb_2O content, a systematic investigation of the local structure around Rb ions was undertaken, with emphasis placed on interatomic distances, coordination numbers, and structural disorder of glass former and modifier cations.[1] The results indicated that no correlation exists between the composition dependence of activation energy and that of the interatomic distances, or the disorder parameters. It was found though that the maximum in E_σ parallels the appearance of a minimum in the ''unoccupied volume'' of the glass.

Greaves and Ngai proposed recently a cooperative ion movement model to derive transport properties from the local atomic structure in single and mixed alkali silicate glasses.[6] The agreement between experimental and calculated transport properties was found to be satisfactory. Therefore, an attempt was made to understand the composition dependence of activation energy in rubidium germanate glasses in terms of the cooperative ion motion model, but considerable discrepancies between calculated and observed activation energies were found.[1] This result led to the proposition that the structural origin of such differences should be traced to the way alkali metal ions are distributed in the glass structure. On the basis of extended x-ray-absorption fine-structure (EXAFS) studies Greaves and co-workers[7,8] showed that the alkali ions in silicate glasses are not distributed homogeneously, but rather they segregate in alkali-rich regions. This structural picture did not seem to apply to Rb-germanate glasses, because the EXAFS and x-ray photoemission spectroscopy (XPS) results indicated that Rb ions are relatively randomly distributed in the structure by comparison with the alkalis in silicate glasses.[9]

It appears, therefore, that the distribution pattern of rubidium cations in the germanate glass structure could be one of the key factors determining the ion transport properties. Investigations of ionically modified glasses by far-infrared spectroscopy have demonstrated the capabilities of this technique in revealing the nature and distribution of anionic sites occupied by metal ions.[10–15] Recent far-infrared studies of alkali borate glasses have shown that alkali metal ions are distributed over two types of sites, and that the mobile cations are mainly those occupying sites of high basicity, i.e., sites with high electron density.[15–17]

In the present work we apply far-infrared spectroscopy to Rb-germanate glasses in an attempt to clarify the nature of sites hosting rubidium ions and their influence on ionic conductivity. To facilitate this investigation, the germanate glasses containing 20 mol % of different alkali oxides were also studied. Activation energies for ionic conductivity were calculated on the basis of the free-ion model[18,19] and compared with experimental values,[1] in order to identify the type of Rb ion sites facilitating the long-range ion movement.

II. EXPERIMENT

Two glass series, $0.20R_2O$-$0.80GeO_2$ (R=Li,Na,K,Rb,Cs) and xRb_2O-$(1-x)GeO_2$ ($0<x\leq 0.27$) were prepared and studied. The first series is employed to investigate the effect of alkali type, and the second the effect of alkali content on the far-infrared spectrum. Appropriate amounts of GeO_2 and alkali metal carbonate powders were thoroughly mixed and melted in platinum crucibles for ~1.5 h at 900–1000 °C, depending on composition. Glass samples were obtained by casting the bubble-free melts in a stainless-steel mold. Rb-germanate glasses with $x=0.0075$, 0.01, 0.02, 0.05, 0.10, 0.15, were prepared from the same batch which was used for the glass samples of EXAFS, XPS, and conductivity studies.[1,3,9] Specimens appropriate for infrared measurements were prepared by cutting and polishing glass samples, to obtain discs of approximate dimensions 1 cm×1 cm×1 mm.

For the purpose of spectral comparisons and assignments, two crystalline compounds of composition $Rb_2Ge_4O_9$ (20 mol % Rb_2O) and $K_4Ge_9O_{20}$ (18.2 mol % K_2O) were also prepared and studied. The first compound was prepared by slow cooling the corresponding melt from 1250 °C to 850 °C, and then letting the melt to stay for 5 h at 850 °C, while the second was obtained by annealing the corresponding glass at 600 °C for 24 h.[20] In both cases, materials were obtained in a polycrystalline form.

Infrared spectra were recorded in the reflectance mode on a Fourier-transform vacuum spectrometer (Bruker 113v) equipped with an 11° off-normal reflectance attachment. Appropriate sources (Hg arc and globar) and detectors (DTGS with polyethylene and KBr windows) were used to cover the entire infrared region. Five Mylar beam splitters of variable thickness (3.5–50 μm) were used in the far infrared and a KBr one in the midinfrared to measure the spectrum of each glass sample. Therefore, six spectral segments, each one corresponding to the optimum beam splitter throughout, were finally merged into one data file to give a continuous reflectance spectrum. The combination of this approach with the good quality of surfaces of the glass samples resulted in high-quality reflectance spectra in the range 20–4000 cm^{-1}. The spectrum of a high-reflectivity aluminum mirror was used as a reference. All spectra were measured with 2-cm^{-1} resolution at room temperature and represent the average of 200 scans. The reflectance data were first extrapolated to frequencies $\nu\rightarrow 0$ and $\nu\rightarrow\infty$, using the Bruker EXTPOLR program, and then were analyzed by employing the Kramers-Kronig (KK) technique.[15] The absorption coefficient spectra reported in this work were calculated from the expression

$$\alpha=4\pi\nu k=2\pi\nu\varepsilon''/n, \tag{1}$$

where ν is the frequency in cm^{-1}. The real (n) and imaginary (k) parts of the refractive index and the imaginary (ε'') part of the complex dielectric permittivity were obtained by the KK analysis and the application of the Fresnel formulas.[15]

III. RESULTS

A. Far-infrared spectra of $0.20R_2O$-0.80 GeO_2 glasses

The absorption spectra of $0.20R_2O$-0.80 GeO_2 glasses are shown in Fig. 1 in the far-infrared region. The midinfrared spectra (500–1300 cm^{-1}) which give information about the structure of the germanate network, will be presented and discussed in detail elsewhere.[21] As shown in Fig. 1 the far-infrared profiles consist of a number of broad and highly overlapping bands. To investigate the origin of such bands and their composition dependence we have analyzed these spectra using a least-squares-fitting program and a deconvolution procedure applied to binary and ternary glasses, including borates, silicates, and phosphates.[12,15–17,22] In this procedure we employ the minimum number of bands that give a reasonable agreement between calculated and experimental spectrum. The final resonance frequencies of the bands, their bandwidth, intensity and functional form, are parameters adjustable by the program.

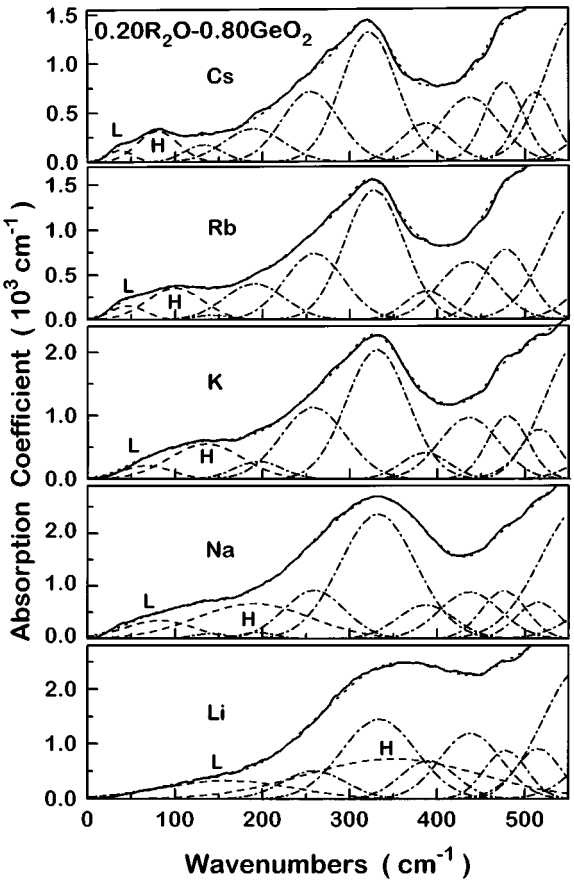

FIG. 1. Far-infrared spectra of $0.20R_2O$-$0.80GeO_2$ (R=Li, Na, K, Rb, Cs) glasses (solid lines) and their deconvolution into Gaussian component bands. The simulated spectra are shown by the dotted lines.

The results of the deconvolution are shown in Fig. 1 and the frequencies of the resulting bands are listed in Table I. It is noted that all bands have almost 100% Gaussian band shape. The frequencies of all bands, but those listed in the last two rows of the table, show very small dependence on the type of alkali ion. Thus, we assign those bands to vibrational modes of the germanate network with little influence from the alkali metal ion. The high-frequency components at ~565, 515, 475, and 435 cm^{-1} are attributed to the bending vibration of Ge-O-Ge bridges, and those at ~390, 335, and 256 cm^{-1} to the rocking motion of the bridging oxygen atom perpendicular to the Ge-O-Ge plane.[23] The weak components

TABLE I. Frequencies (cm^{-1}) and assignments of component bands obtained by deconvolution of the far-infrared spectra of $0.20R_2O$-$0.80GeO_2$ glasses (R=Li, Na, K, Rb, Cs).

Li	Na	K	Rb	Cs	Assignment
564	565	564	564	560	
515	515	516	513	512	Ge-O-Ge
478	476	480	478	476	bending
438	437	436	435	437	
390	387	386	388	387	
334	332	331	327	322	Ge-O-Ge
259	259	258	259	255	rocking
	195	195	190	190	Network
	140		142	132	torsion
350	190	135	100	80	Alkali ion
160	82	67	46	37	motion

at ~140 and 190 cm^{-1} are assigned to torsion modes of the germanate network.[24] The presence of more than one band for each type of vibrational mode can be due to the existence of a distribution of Ge-O-Ge angles as a result of the presence of germanate rings of various sizes.[25]

The frequencies listed in the last two rows of Table I and marked by L and H in Fig. 1, show large dependence on the type of alkali ion. When plotted versus the inverse of the square root of the corresponding cation mass (Fig. 2) show a linear dependence on $M_c^{-1/2}$, where M_c is the mass of alkali cation. On this basis, we assign the L and H bands, with frequencies ν_L and ν_H, respectively, to vibrations of alkali cations in two types of anionic environments and/or sites (sites L and H), in analogy with our previous findings in alkali borate glasses.[15–17] The quite linear dependence of $\nu_{H(L)}$ on $M_c^{-1/2}$ does not necessarily mean that M_c is the correct reduced mass, μ, of the vibration, because it involves also motion of the oxygen atoms which constitute the anionic site.[14,15] This is in order for the center of mass of the site and/or cage to remain fixed during vibration. Therefore, Fig. 2 implies only that the alkali ion vibrates against a quite rigid anionic site. Considering the fact that the oxygen atoms of the site are not free but bonded to germanium atoms in large and massive network arrangements, the approximation $\mu \approx M_c$ seems to be very reasonable.[13] The relative integrated intensity of the low-frequency component band, $A_L/(A_L+A_H)$, is shown in the inset of Fig. 2. Clearly, $A_L/(A_L+A_H)$ decreases progressively from Li to Cs.

The H bands of the K-germanate and Rb-germanate glass spectra form the envelope of the infrared-active phonon bands of the corresponding $K_4Ge_9O_{20}$ and $Rb_2Ge_4O_9$ crystal spectra. This is demonstrated in Fig. 3, where glass and crystal spectra are compared. As shown in the same figure, the L bands of the glass spectra appear to have no counterpart in the crystal spectra. This suggests that L bands correspond to an additional distribution of phonon states in the glassy forms of the materials.

B. Far-infrared spectra of xRb_2O-$(1-x)GeO_2$ glasses

The far-infrared spectra of xRb_2O-$(1-x)GeO_2$ glasses, for Rb_2O contents spanning the range $0<x\leq 0.25$, are shown in Fig. 4 in an expanded frequency and intensity scale. These

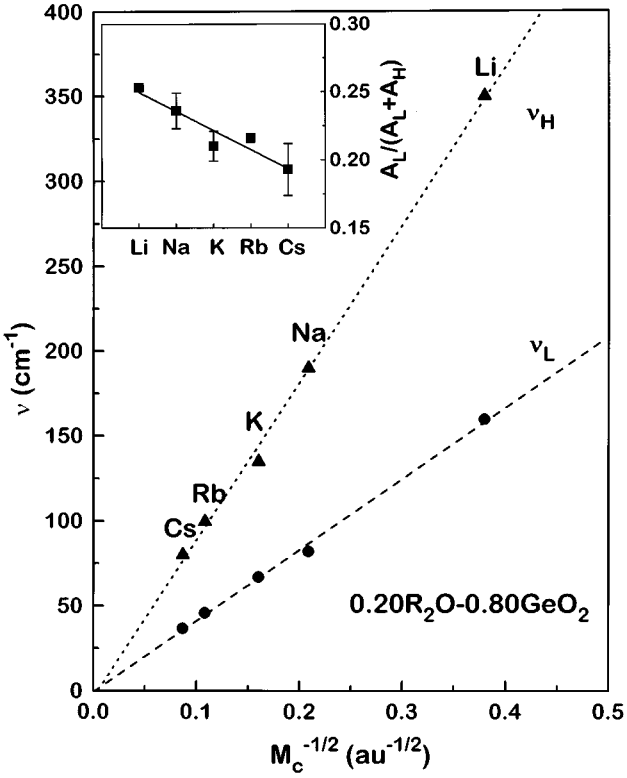

FIG. 2. Cation-motion frequencies vs $M_c^{-1/2}$, where M_c is the mass of alkali cation. ν_L and ν_H denote the low- and high-frequency maxima resulted from the deconvoluted spectra shown in Fig. 1. The inset shows the alkali cation dependence of the relative integrated intensity, $A_L/(A_L+A_H)$, of the low-frequency ion motion band. Lines are least-squares fittings to the data. Error bars of frequencies are within the size of symbols.

spectra were deconvoluted into Gaussian components as described above. While the frequencies of the bands above ~150 cm^{-1} remain practically constant, their relative intensities vary with Rb_2O content, indicating a systematic modification of the germanate lattice upon adding alkali oxide.

Of particular interest are the results concerning the parts of the spectra below ~130 cm^{-1} (dashed lines in Fig. 4); for $x>0.075$ two bands (marked by L and H) were deconvoluted, while for $x\leq 0.075$ one component (marked by M) could be resolved. The integrated intensities of the L, M, and H bands have been normalized relative to the total integrated intensity of the spectrum in the range 0–500 cm^{-1}, and the results are presented in Fig. 5(a). The linear increase of the relative intensities with rubidium oxide content supports the assignment of all three bands to Rb ion motion in the corresponding network sites. Figure 5(b) illustrates the composition dependence of the relative intensity $A_{L(M)}/(A_{L(M)}+A_H)$. Because of the presence of only one band (M) for $x\leq 0.075$ the relative integrated intensity equals one in this composition range, and then decreases drastically for $0.075<x\leq 0.125$ because of the presence of two bands. For $x\geq 0.125$, the relative intensity $A_L/(A_L+A_H)$ remains practically constant.

The composition dependence of the frequencies ν_L, ν_M, and ν_H of bands L, M, and H, respectively, is shown in Fig. 6(a). The three frequencies increase almost linearly upon increasing the Rb_2O content, and ν_M shows the largest rate of

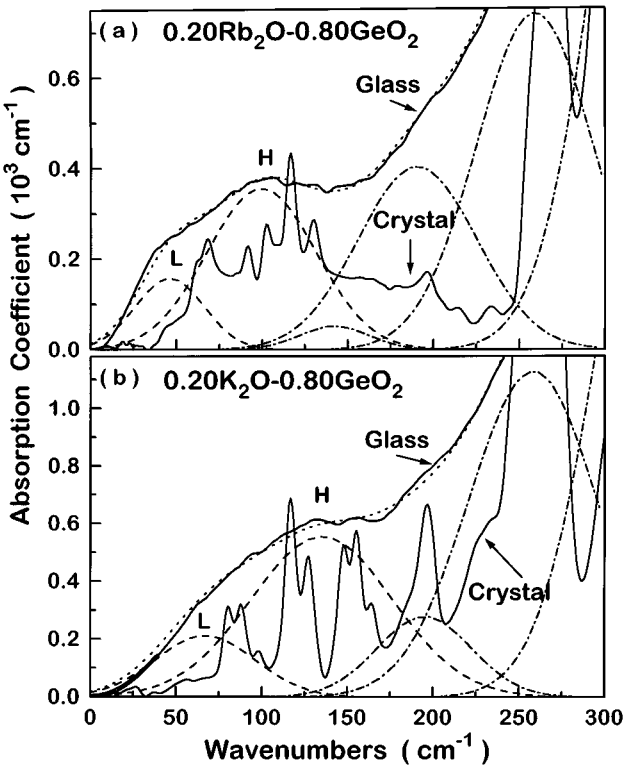

FIG. 3. Comparison between the far-infrared spectra of $0.20R_2O$-$0.80GeO_2$ (M=Rb, K) glasses with those of the crystalline compounds $Rb_2Ge_4O_9$ (a) and $K_4Ge_9O_{20}$ (b), having the same (R=Rb) or similar (R=K) alkali content.

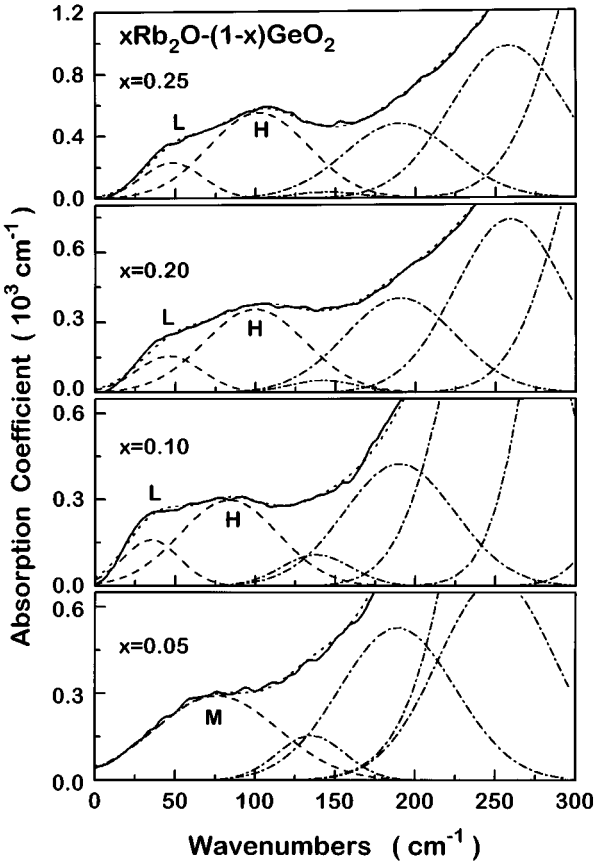

FIG. 4. Deconvoluted far-infrared spectra of xRb_2O-$(1-x)GeO_2$ glasses (solid lines) into Gaussian components. The simulated spectra are also shown (dotted lines).

increase with x. The relative bandwidths, $\Delta\nu/\nu$, of the three bands are plotted versus Rb_2O content in Fig. 6(b) ($\Delta\nu$=full width at half maximum and $\nu=\nu_L$, ν_M, and ν_H). For all bands the relative bandwidth, $\Delta\nu/\nu$, decreases with x. If we consider $\Delta\nu/\nu$ as a measure of the disorder of sites hosting Rb ions,[26] then the data in Fig. 6(b) suggest that H bands should originate from vibrations of Rb ions in relatively more ordered, or crystal like sites. Also, M-type sites tend to become H like sites at a faster rate than the L sites do.

IV. DISCUSSION

A. The nature of alkali metal sites in germanate glasses

1. Comparison between the far-infrared spectra of crystalline and glassy phases

It is illustrated in Fig. 3 that the H band of the glass spectrum forms the envelope of the absorption profile in the same frequency range of the crystal with the same or similar composition. Therefore, it should be possible to reveal the nature of M, L, and H sites in glass if we understand the origin of the corresponding peaks of the crystalline phases for which the structure is known.

$Rb_2Ge_4O_9$ crystallizes trigonally with space group $P\bar{3}c1$ (D^4_{3d}) and has six molecules in the unit cell.[27,28] The 12 Rb ions in the cell are located on sites with symmetry C_1 and are sevenfold coordinated to oxygen atoms. Six of the Rb-O distances are in the range 2.82–2.93 Å and the seventh oxygen is located 2.99 Å apart. For the sake of simplicity and in order to make possible the comparison between crystal and glass spectra we assume that Rb ions in the glass occupy octahedral, O_h, sites. This assumption is supported by the EXAFS results which give an average rubidium coordination number around six.[9] For sites of O_h symmetry group theory predicts that there is only one infrared-active Rb-O_6 stretching vibration corresponding to the triply degenerate T_{1u} mode. The situation is different in the crystal, because the presence of Rb ions on C_1 sites in a crystal field of D_{3d} symmetry causes the removal of degeneracy of the T_{1u} modes, and hence the appearance of additional bands in the crystal spectrum.

The type and number of modes arising from Rb-site vibrations in the $Rb_2Ge_4O_9$ crystal can be obtained by factor group analysis,[29] as shown schematically in Table II, where point group C_{2h} was utilized to facilitate correlation between C_1 and D_{3d}. After subtracting the three acoustic modes ($1A_{2u}+2E_u$) from the total number of Rb^+ translatory modes the following representation is obtained:

$$\Gamma_{\mathrm{Rb}}=3A_{1g}(R)+3A_{2g}(\mathrm{ia})+6E_g(R)+3A_{1u}(\mathrm{ia})+2A_{2u}(\mathrm{IR})+4E_u(\mathrm{IR}), \quad (2)$$

where R, ia, and IR denote a Raman-active, inactive, and an infrared-active modes, respectively. The above expression predicts nine Raman-active ($3A_{1g}+6E_g$), and six infrared active ($2A_{2u}+4E_u$) modes arising from Rb ion motion in the crystal. On the basis of this factor group analysis, we

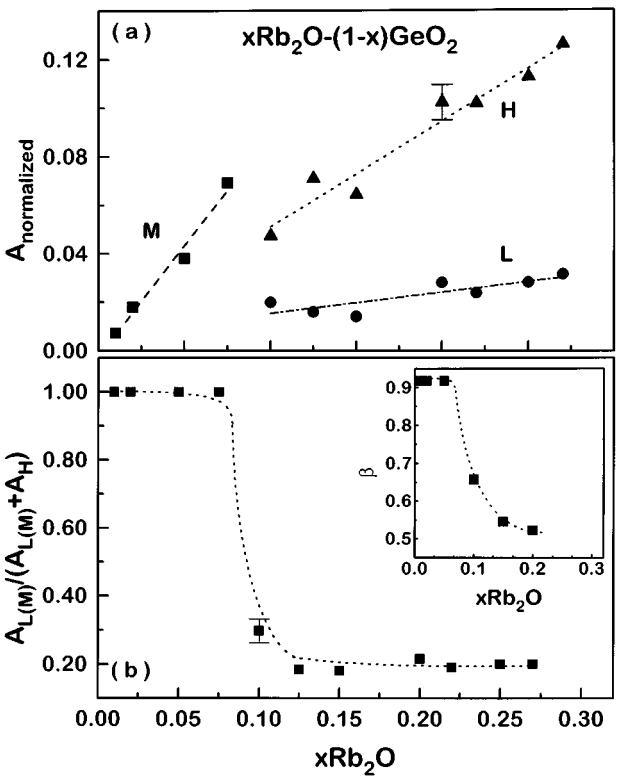

FIG. 5. (a) Composition dependence of the normalized integrated intensities of bands L, M, and H obtained by deconvoluting the far-infrared spectra of $x\mathrm{Rb_2O}$-$(1-x)\mathrm{GeO_2}$ glasses (Fig. 4), and (b) variation of the relative integrated intensity $A_{L(M)}/(A_{L(M)}+A_H)$ with $\mathrm{Rb_2O}$ mole fraction in the same glasses. The inset of (b) shows the composition dependence of the Kohlrausch exponent β for the same glasses (Ref. 3). Lines are drawn to guide the eye.

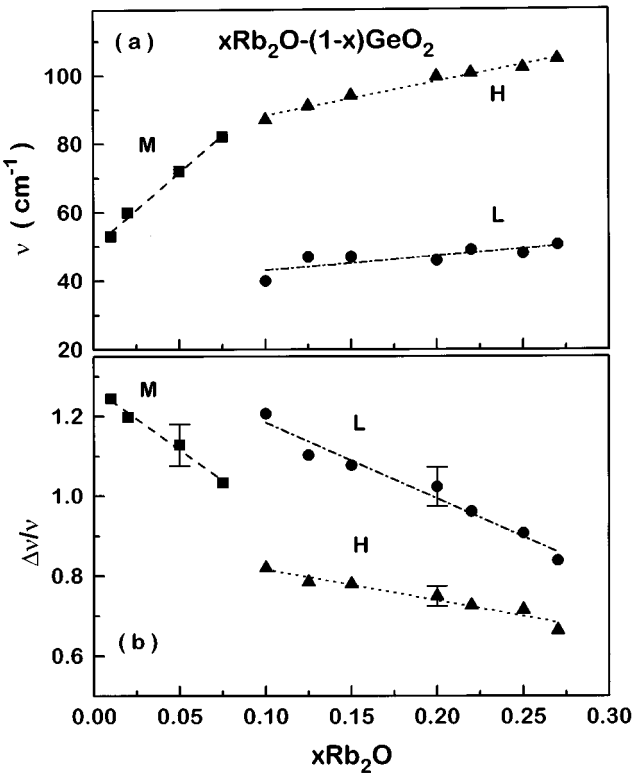

FIG. 6. Composition dependence of the frequencies (a), and of the relative bandwidths (b), of rubidium motion bands L, M, and H, obtained from the deconvoluted far infrared spectra of $x\mathrm{Rb_2O}$-$(1-x)\mathrm{GeO_2}$ glasses. Lines are drawn to guide the eye (for details see text).

assign the six peaks of the crystal spectrum at 63, 68, 92, 102, 107, and 130 cm^{-1} to the $2A_{2u}$ and $4E_u$ predicted modes. As shown in Fig. 3 all six Rb motion peaks in the crystal are within the H band envelope of the glass. It is, therefore, appropriate to assign the H band of glass to the T_{1u} mode of Rb ion motion in crystal-like O_h sites.

The crystal structure of $\mathrm{K_4Ge_9O_{20}}$ is similar to that of $\mathrm{Na_4Ge_9O_{20}}$: space group $I41/\alpha$ (C_{4h}^6) with four formula units in the unit cell.[30,31] The 16 alkali ions occupy sites of C_1 symmetry and are sixfold coordinated by oxygen atoms. EXAFS studies of K-germanate glasses showed that K ions are also on the average sixfold coordinated in the glass.[32] We can thus assume O_h symmetry for the sites of K ions in glass, which leads to the T_{1u} mode of K ion motion. A prediction of the corresponding modes in the field of the $\mathrm{K_4Ge_9O_{20}}$ crystal can be made on the basis of the factor group analysis summarized in Table III. It leads to the following representation for the K^+ translatory modes:

$$\Gamma_K = 6A_g(R) + 6B_g(R) + 6E_g(R) + 5A_u(\mathrm{IR}) + 6B_u(\mathrm{ia}) + 4E_u(\mathrm{IR}) \quad (3)$$

after subtracting the acoustic modes, one of A_u symmetry and two of E_u symmetry. Thus, factor group analysis predicts nine infrared-active modes ($5A_u+4E_u$) for the K ion motion in the field of the $\mathrm{K_4Ge_9O_{20}}$ crystal. Inspection of Fig. 3 shows eight well-resolved peaks at 80, 88, 97, 117, 127, 148, 155, and 165 cm^{-1} under the envelope of the H band, in very good agreement with theory. A shoulder observed at 185 cm^{-1} could correspond to the ninth mode of K ion motion in the crystal.

2. Effect of alkali type and content on the nature and distribution of metal ion sites

It is evident from the comparison of crystal and glass spectra that the H band of glasses can be assigned to vibrations of metal ions in sites similar to those found in the corresponding crystalline compounds. The local geometry around metal ions in germanate glasses can be considered as being nearly octahedral, O_h. The possibility though exists that Li^+ ions in germanate glasses of high alkali content may occupy sites nearly tetrahedral, T_d, symmetry.[33] Cation motion in a tetrahedral site gives rise also to a triply degenerate, T_2, infrared-active mode,[14] the degeneracy of which can be removed by the influence of the crystal field.

We have argued elsewhere[17,26] that during the glass-forming process the synergy between site requirements for the metal cations and site provisions by the glass network could lead to the establishment of well-defined sites for the cations. In particular, as the melt of the glass is cooled thermodynamics drives the system to the stable crystalline state, but kinetics does not allow it to reach the crystalline structure. Therefore, the natural tendency of the alkali ions is to situate themselves in crystal-like site, and in fact some alkali ions succeed in achieving this goal. It is the vibration of

TABLE II. Correlation diagram between point group, site group, and unit-cell group for the Rb ion motion modes in crystalline and glassy $Rb_2Ge_4O_9$. In the crystal there are six molecules per unit cell, i.e., 12 Rb ions. Note that numbers in parentheses indicate the number of modes.

Glass Point group	Crystal Site group		Factor group
O_h	C_1	C_{2h}	D_{3d}
			$A_{1g}(3)$ R
		$A_g(9)$	$A_{2g}(3)$ ia
		$B_g(9)$	$E_g(6)$ R
$T_{1u}(12)$	$A(36)$		
		$A_u(9)$	$A_{1u}(3)$ ia
		$B_u(9)$	$A_{2u}(3)$ IR
			$E_u(6)$ IR

TABLE III. Correlation diagram between point group, site group, and unit-cell group for the K ion motion modes in the crystalline and glassy phase of $K_4Ge_9O_{20}$. In the crystal there are four formula units per unit cell, i.e., 16 K ions in the cell. Note that numbers in parenthesis indicate the number of modes.

Glass Point group	Crystal Site group		Factor group
O_h	C_1	C_{2h}	C_{4h}
			$A_g(6)$ R
		$A_g(12)$	$B_g(6)$ R
		$B_g(12)$	$E_g(6)$ R
$T_{1u}(16)$	A (48)		
		$A_u(12)$	$A_u(6)$ IR
		$B_u(12)$	$B_u(6)$ ia
			$E_u(6)$ IR

metal ions in such type of sites that gives rise to the far-infrared H bands in glasses. As the melt cools further the atom movement becomes sluggish and yet a fraction of alkali ions have not established stable sites for themselves. Such alkali ions occupy energetically less favorable sites, or ''secondary'' sites, where anionic charge density and coordination number do not have their optimum values. Larger coordination numbers, i.e., larger cation-oxygen distance, and smaller charge density of site than the optimum values are factors that both result in smaller ion motion frequencies.[14] This effect can be easily understood on the basis of the following expression which gives the ion motion frequency, ν:

$$\nu^2=[\alpha/48\pi^3c^2\varepsilon_0][(r_0/\rho)-2][q_Cq_A/\mu r_0^3] \qquad (4)$$

in terms of the charges of cation, q_C, and site, q_A, the reduced mass of vibration, μ, and the cation-oxygen distance r_0.[14] α is the pseudo-Madelung constant, c is the speed of light, ε_0 is the permittivity of free space, and ρ is the repulsion parameter of the Born-Mayer potential. Therefore, we assign the L bands in the glass spectra to vibrations of metal ions in ''secondary'' sites, the existence of which is responsible for the extra absorption exhibited by glasses at low frequencies (below the H bands) as compared to crystals.

The presence of two ion motion bands (L and H) is not a characteristic of alkali germanate glasses alone. It was found to be the case in other ionically modified glasses as well, including borates, silicates, molybdates, and phosphates.[12–17,22] Thus, the picture emerging from the far-infrared study lends support to earlier suggestions for an inhomogeneous distribution of alkali metal ions in the glass structure.[7,8,12,34–37] Assuming that the presence of the two ion motion bands (L,H) is a manifestation of an energetically inhomogeneous distribution of the alkali ions, the inset of Fig. 2 shows that the distribution of larger alkali ions in the glass structure is relatively more homogeneous.

While the two bands (L and H) characterize Rb-germanate glasses with relatively high alkali contents ($x>0.075$), only one band was required to simulate the spectra for $x\leqslant 0.075$ (Fig. 4). Thus, in the low alkali range ($x\leqslant 0.075$) Rb ions are distributed over one type of site (M), which is probably the precursor of the H sites. When the Rb_2O content exceeds a certain limit ($x\approx 0.075$) only then the H sites are formed. The relative population of H sites increases in the composition range $0.10<x<0.125$, and then it remains almost constant for higher rubidium oxide contents [Fig. 5(b)].

It is of interest to note at this point that the composition dependence of the relative population of cation sites shown in Fig. 5(b) is very similar to that of the Kohlrausch exponent, β, for electrical relaxation in Rb-germanate glasses, depicted in the inset of Fig. 5(b).[3] It was found that β is nearly equal to one ($\beta=0.93$) for $x\leqslant 0.05$, decreases progressively to the value $\beta=0.55$ at $x=0.15$ and then stays almost constant up to $x=0.25$. Previous attempts to explain the variation of β with composition have made correlations of β with a range of macroscopic glass properties including, the magnitude of conductivity, the decoupling index, the activation energy of conductivity and the nominal cation-cation distance (for a survey of previous works on correlations of β see Ref. 3). Each correlation was found to have limited validity. The results of this work suggest that one structural cause for the decrease of β, i.e., the further broadening of the peak of the imaginary part of electric modulus, M'', could be the development of a new distribution of sites (H) for the alkali ions when $x>0.075$. Similarly, Greaves and Ngai[6] have associated the decrease of β in silicate glasses with the establishment of alkali clusters in the structure.

When the Rb_2O content increases, the resonance frequencies (ν_L, ν_M, and ν_H) of all three Rb motion bands increase [Fig. 6(a)]. Assuming that the reduced mass of Rb vibration remains constant, $\mu\approx M_{\mathrm{Rb}}$, the increase of ν can result from the increase of q_A and/or the decrease of r_0 [see Eq. (2)]. XPS, Raman, and infrared studies of the same glasses have shown that addition of Rb_2O to GeO_2 results in the formation of negatively charged units; the $Ge\emptyset_6^{2-}$ octahedra prevail in the range $0<x<0.15$ ($\emptyset$ is the bridging oxygen), while germanate tetrahedra with nonbridging oxygens, $Ge\emptyset_{4-n}O_n^{n-}$, are formed at high rates for further Rb_2O additions.[9,21] Furthermore, the EXAFS results indicate that the average Rb-O distance decreases slightly with increasing amount of Rb_2O in the glass.[9] It is obvious that these progressive structural changes are registered by Rb ions which vibrate at systematically higher frequencies as shown in Fig. 6(a).

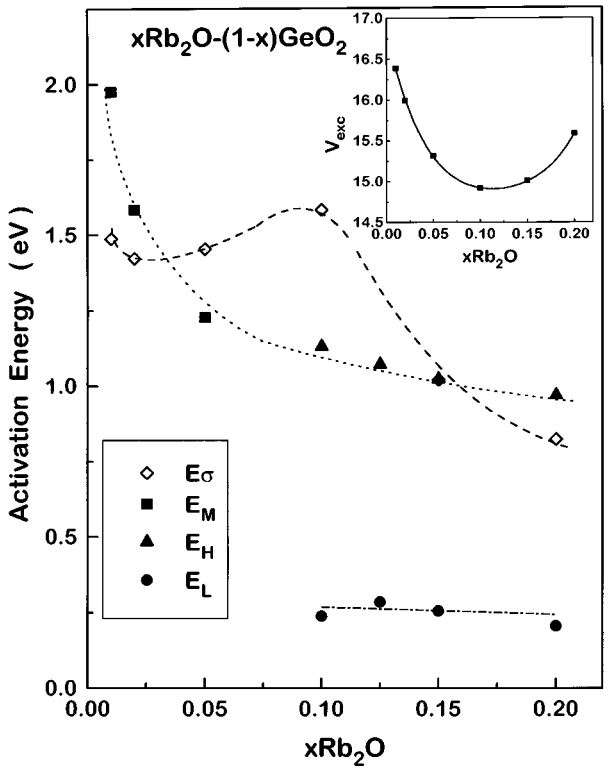

FIG. 7. Activation energy for dc ionic conductivity vs Rb_2O mole fraction in xRb_2O-$(1-x)GeO_2$ glasses. The experimental activation energies, E_σ, are compared with values calculated in this work on the basis of the ion-free model (E_M, E_H, and E_L). The inset shows the ''excess volume'' $V_{\rm exc}$ (in cm^3/mol), for the same glasses. Lines are drawn to guide the eye.

B. Conductivity activation energies from far-infrared data

Since the nature and distribution of the Rb ion-hosting sites have been established in the previous sections, it appears tempting to find a structural basis for the composition dependence of ionic conductivity. Figure 7 shows the experimental activation energy, E_σ, for dc conductivity as a function of Rb_2O content.[1] A maximum of E_σ at $\sim$10 mol % Rb_2O is well pronounced.

It was shown above that changes in the distribution of Rb ions are manifested by changes in the ion oscillation frequencies in the far infrared. A model which places special emphasis on the mobile ion oscillation frequency is the free-ion model of Rice and Roth, introduced to describe ionic conduction in crystalline superionic conductors.[18] According to this model, an energy gap, E_0, exists above which the mobile ion of mass M_c can be thermally excited from its localized ionic state to free-ion-like states. In the mth excited state the ion propagates with velocity $\mathbf{v}_m$ and energy $E_m=(M_c\mathbf{v}_m^2)/2$. Because of the interactions with the rest of the solid the ion in the excited state loses energy and returns eventually to its localized state. The excited state is characterized by a lifetime, τ_m, during which the mobile ion travels a mean-free path, l_m, given by $l_m=\mathbf{v}_m\tau_m$. Rice and Roth then showed that the ionic conductivity is given by

$$\sigma=[(Ze)^2 n\mathbf{v}_0 l_0/3kT]\exp(-E_0/kT), \tag{5}$$

where Ze is the charge of the mobile ion, n is the number of mobile ions per unit volume, and $E_0, l_0, \mathbf{v}_0, \tau_0$, characterize the free-ion state at the energy gap. They noted that the above expression becomes equivalent to the Arrhenius expression for the ion hopping model[38] when $\mathbf{v}_0 l_0$ is replaced by $d^2\nu_0$, where d is the ion hopping, or jump distance and ν_0 is the ionic oscillator frequency. Then the energy gap E_0 is identified with E_σ, the mean-free path l_0 with d, and the inverse lifetime $1/\tau_0$ with ν_0. Therefore, the energy of the mobile ion at the energy gap, $E_0=(M_c\mathbf{v}_0^2)/2$, can be rewritten in the form

$$E_\sigma=(M_c d^2\nu_0^2)/2. \tag{6}$$

The above equation yielded values of E_σ for crystalline ionic conductors in good agreement with experimental values.[18]

Exarhos *et al.*[19] applied the Rice and Roth model to ionic glasses and were able to derive the same energy expression as for the crystalline conductors [Eq. (6)]. Activation energies calculated for alkali metaphosphate and silicate glasses,[19] as well as for alkali borate glasses,[39] were found to be in reasonable agreement with the experimental values.

We apply here the free-ion model to Rb-germanate glasses for which the ion oscillation frequencies have been determined. Accurate values of the ion jump distance, d, are difficult to obtain even for crystalline ionic conductors;[40] for glasses this difficulty is enhanced. We proceed by equating d with the average Rb-Rb distance, obtained by assuming a homogeneous distribution of the ions. Then, $d=(V_m/2xN_A)^{1/3}$ where V_m is the molar volume of the glass given in Table IV,[1] N_A is Avogadro's number, and x is the mole fraction of Rb_2O. Since three Rb motion frequencies (ν_L, ν_M, and ν_H) are obtained from the far-infrared analysis, three activation energies (E_L, E_M, and E_H) are calculated assuming that Rb ions in all types of sites contribute to ionic conduction.

The calculated activation energies are compared in Table IV with the experimental results, E_σ, and plotted in Fig. 7 versus Rb_2O content. Several observations can be made; first, it is observed that E_H provides a smooth continuation of the composition dependence of E_M. This result reinforces the suggestion made earlier that M sites are the precursors of H sites. Second, there is a hint for a small hump at $\sim x=0.075$, but this is far from being a maximum in the activation energy. Third, the activation energies calculated from frequencies ν_L are in obvious disagreement with the experimental results. This observation is in agreement with our previous results for alkali borate glasses that the mobile alkali ions are those which occupy H sites.[16–17] Therefore, conduction pathways seem to be established probably along high-frequency sites, which resemble the sites formed in the analogous crystalline compounds.

The largest difference between E_σ and E_M/E_H is observed at $\sim$10 mol % Rb_2O (Fig. 7). At this composition the ''unoccupied volume,'' or the ''excess volume,'' $V_{\rm exc}$, of the glass passes through a minimum as shown in the inset of Fig. 7. It is noted that $V_{\rm exc}$ may be considered as the volume of the glass that is not occupied by any atoms, and therefore may represent the available space for the diffusion of mobile ions.[1] This suggests that the difference between E_σ and calculated activation energy at $\sim$10 mol % Rb_2O most likely arises from the fact that the strain part of the activation energy, in terms of the Anderson and Stuart model,[41] is not accounted for by the free-ion model.

TABLE IV. Values of molar volume V_m, jump distance d, and experimental activation energy of dc conductivity E_σ for $x\mathrm{Rb_2O}$-$(1-x)\mathrm{GeO_2}$ glasses. Calculated activation energies E_M, E_H, and E_L, from the free-ion model using frequencies ν_M, ν_H, and ν_L, are also given.

x	V_m[a] ($\mathrm{cm^3}$)	d (Å)	E_σ[a] (eV)	E_M (eV)	E_H (eV)	E_L (eV)
0.01	28.25	13.28	1.488	1.98		
0.02	27.95	10.51	1.423	1.59		
0.05	27.60	7.71	1.455	1.23		
0.075	27.62[b]	6.74	-	1.20		
0.10	27.69	6.12	1.584		1.14	0.24
0.125	27.88[b]	5.70	-		1.07	0.29
0.15	28.30	5.39	1.021		1.02	0.26
0.20	29.37	4.95	0.817		0.97	0.21

[a]Reference 1.
[b]From interpolation.

The strain part of the activation energy would be maximum at ~10 mol % $\mathrm{Rb_2O}$ where V_{exc} is minimum. When the alkali oxide content increases above 10 mol %, V_{exc} of glass increases (Fig. 7), and thus the effect of the strain energy on E_σ will decrease. Along these lines, we expect a better agreement between E_σ and calculated activation energy for such glass compositions, as shown clearly in Fig. 7. We consider also the $0.20R_2\mathrm{O}$-$0.80\mathrm{GeO_2}$ glasses (R=alkali), and compare in Table V experimental activation energies for ionic conductivity, E_σ, with calculated ones on the basis of the free-ion model. These are the E_H energies obtained by employing the high frequencies, ν_H, of cations R, given in Table I. Clearly, the agreement between E_σ and E_H has been improved considerably, stressing the importance of the strain energy part of the activation energy for ion transport.

V. CONCLUSIONS

The nature and distribution of sites hosting alkali metal ions in germanate glasses has been investigated by infrared reflectance spectroscopy as a function of alkali type and content. The analysis of the far-infrared spectra of glasses with fixed alkali content, $0.20R_2\mathrm{O}$-$0.80\mathrm{GeO_2}$ (M=Li, Na, K, Rb, Cs), revealed the presence of two distributions of ionic sites characterized by low (L) and high (H) frequencies of the cation motion modes, besides the presence of bands arising from germanate network modes. The far-infrared spectra of glasses were compared with those of corresponding crystalline compounds, and factor group analysis was performed to deduce the cation motion modes in the field of the crystal. It was found that the H band of glass spectra can be assigned to the T_{1u} mode in nearly octahedral sites in the glass, and that it constitutes the envelope of the ion motion modes in the crystal. The L bands of glass spectra represent additional absorption in glass as compared to crystals and can be attributed to ion motion in ''secondary'' sites, where coordination numbers and anionic charge density have not reached yet their optimum values established in the crystal, or those values characterizing crystal-like H sites.

TABLE V. Values of molar volume V_m, jump distance d, experimental activation energy of dc conductivity E_σ, and calculated activation energy E_H from the free-ion model using ν_H frequencies, for $0.20R_2\mathrm{O}$-$0.80\mathrm{GeO_2}$ glasses (R=Li, Na, K, Rb, Cs).

R	V_m ($\mathrm{cm^3}$)	d (Å)	E_σ (eV)	E_H (eV)
Li	22.10[a]	4.51	0.79[a]	0.81
Na	23.86[b]	4.63	0.87[c]	0.83
K	27.02[b]	4.82	0.82[d]	0.77
Rb	29.30[b]	4.95	0.82[d]	0.98
Cs	31.93[b]	5.10	-	1.03

[a]Reference 4.
[b]Reference 42.
[c]Reference 5.
[d]References 1 and 3.

From the study of germanate glasses of variable alkali content, $x\mathrm{Rb_2O}$-$(1-x)\mathrm{GeO_2}$ ($0<x\leqslant 0.27$), it was found that for $x\leqslant 0.075$ only one Rb motion band at intermediate frequencies (M) is required to simulate the low-frequency parts of the far-infrared spectra. When the $\mathrm{Rb_2O}$ content exceeds a minimum value ($x\approx 0.10$) the formation of H sites takes place, and the far-infrared spectra show the presence of both H and L bands. The frequencies of all Rb motion bands were found to increase with $\mathrm{Rb_2O}$ content, which is attributed to the increase of anionic charge density of the Rb-hosting sites and to the progressive decrease of the Rb-O distance. The change of the relative population of Rb sites was qualitatively correlated with the composition dependence of the Kohlrausch β exponent.

Finally, the Rice and Roth free-ion model was applied to Rb-germanate glasses to calculate activation energies for conductivity. It was found that although the activation energies calculated from the Rb oscillation frequencies in M and H sites are comparable with the observed values, there remains a qualitative disagreement between the composition dependencies of the two. This discrepancy is most likely due to the fact that the strain part of the activation energy is not incorporated in the free-ion model.

ACKNOWLEDGMENTS

The authors wish to thank the NATO Collaborative Research Grants Program (Grant No. CRG 931213), NHRF and US DOE for supporting this work, and Dr. G. D. Chryssikos and Dr. M. A. Karakassides for helpful discussions.

*Corresponding author; FAX: 30-1 724 9483, electronic address: eik@apollon.servicenet.ariadne-t.gr

[1] W. C. Huang and H. Jain, J. Non-Cryst. Solids **188**, 254 (1995).
[2] J. N. Mundy and G. L. Jin, Solid State Ion. **24**, 263 (1987).
[3] H. Jain and W. C. Huang, J. Non-Cryst. Solids **172-174**, 1334 (1994).
[4] J. E. Shelby and J. Ruller, Phys. Chem. Glasses **28**, 262 (1987).
[5] J. N. Mundy and G. L. Jin, Solid State Ion. **21**, 305 (1986).
[6] G. N. Greaves and K. L. Ngai, J. Non-Cryst. Solids **172-174**, 1378 (1994).
[7] G. N. Greaves, A. Fontain, P. Lagarde, D. Raux, and S. J. Gourman, Nature **293**, 611 (1981).

[8] G. N. Greaves, J. Non-Cryst. Solids **71**, 203 (1985).
[9] W. C. Huang, H. Jain, and M. A. Marcus, J. Non-Cryst. Solids **180**, 40 (1994).
[10] G. J. Exarhos, P. J. Miller, and W. M. Risen, J. Chem. Phys. **60**, 4145 (1974).
[11] B. N. Nelson and G. J. Exarhos, J. Chem. Phys. **71**, 2739 (1979).
[12] E. I. Kamitsos, M. A. Karakassides, and G. D. Chryssikos, J. Phys. Chem. **91**, 5807 (1987).
[13] C. I. Merzbacher and W. B. White, Am. Mineral. **73**, 1089 (1988).
[14] E. I. Kamitsos, J. Phys. Chem. **93**, 1604 (1989).
[15] E. I. Kamitsos, A. P. Patsis, and G. D. Chryssikos, J. Non-Cryst. Solids. **152**, 246 (1993).
[16] J. A. Duffy, E. I. Kamitsos, G. D. Chryssikos, and A. P. Patsis, Phys. Chem. Glasses **34**, 153 (1993).
[17] E. Kamitsos, G. D. Chryssikos, A. Patsis, and J. A. Duffy, J. Non-Cryst. Solids **196**, 249 (1996).
[18] M. J. Rice and W. L. Roth, J. Solid State Chem. **4**, 294 (1972).
[19] G. J. Exarhos, P. J. Miller, and W. M. Risen, Solid State Commun. **17**, 29 (1975).
[20] T. Furukawa and W. B. White, J. Mater. Sci. **15**, 1648 (1980).
[21] E. I. Kamitsos, Y. D. Yiannopoulos, M. A. Karakassides, G. Chryssikos, and H. Jain, J. Phys. Chem. **100**, 11 755 (1996).
[22] E. I. Kamitsos, J. A. Kapoutsis, G. D. Chryssikos, J. M. Hutchinson, A. J. Pappin, M. D. Ingram, and J. A. Duffy, Phys. Chem. Glasses **36**, 142 (1995).
[23] G. Lucovsky, Philos. Mag. **39**, 513 (1979).
[24] H. Verweij and J. H. J. M. Buster, J. Non-Cryst. Solids **34**, 81 (1979).
[25] G. S. Henderson and M. E. Fleet, J. Non-Cryst. Solids **134**, 259 (1991).
[26] E. I. Kamitsos, G. D. Chryssikos, A. P. Patsis, and M. A. Karakassides, J. Non-Cryst. Solids **131-133**, 1092 (1991).
[27] H. Vollenkle and A. Wittmann, Mh. Chem. **102**, 1245 (1971).
[28] M. Goreaud and B. Raveau, Acta Crystallogr. Sect. B **32**, 1536 (1967).
[29] E. B. Wilson, J. V. Decius, and P. C. Cross, *Molecular Vibrations, The Theory of Infrared and Raman Vibrational Spectra* (McGraw-Hill, New York, 1955), pp. 333–340.
[30] N. Ingri and G. Lundgren, Acta Chem. Scand. **17**, 617 (1963).
[31] M. Fleet, Acta Crystallogr. Sect. C **46**, 1202 (1990).
[32] W. C. Huang, H. Jain, and G. Meitzner, J. Non-Cryst. Solids **196**, 155 (1996).
[33] H. Vollenkle and A. Wittmann, Z. Kristallogr. **128**, 66 (1968).
[34] C. Huang and A. N. Cormack, J. Chem. Phys. **95**, 3634 (1991).
[35] H. Melman and S. H. Garofalini, J. Non-Cryst. Solids **134**, 107 (1991).
[36] T. F. Soules, J. Chem. Phys. **71**, 4570 (1979).
[37] A. A. Tesar and A. K. Varshneya, J. Chem. Phys. **87**, 2986 (1987).
[38] A. B. Lidiard, *Handbuch der Physik* (Publisher, City, 1957), Vol. 20, p. 246.
[39] E. I. Kamitsos, M. A. Karakassides, and G. D. Chryssikos, Solid State Ion. **28-30**, 687 (1988).
[40] H. L. Tuller, D. P. Button, and D. R. Uhlmann, J. Non-Cryst. Solids **40**, 93 (1980).
[41] O. L. Anderson and D. A. Stuart, J. Am. Ceram. Soc. **37**, 573 (1954).
[42] J. E. Shelby, J. Appl. Phys. **50**, 276 (1979).